JOURNAL OF COMPUTATIONAL PHYSICS 117, 55–66 (1995)

Finite Difference Method for Calculating Magnetic Field Components Off-Median Plane Using Median Plane Field Data*

DONG-O JEON

National Superconducting Cyclotron Laboratory, Michigan State University, East Lansing, Michigan 48824-1321

Received May 25, 1993; revised May 18, 1994

Given a magnet with midplane symmetry, the field is totally determined if one knows the field in the midplane. A new finite difference method for calculating the field from discrete data in the midplane is described. Because data to be processed are obtained from measurements with noise, the method for evaluating derivatives is required to suppress the high frequency signals effectively, while maintaining reasonable accuracy for low frequencies. First-order and second-order differentiators for a uniform mesh are designed. As a test, they are applied to the magnetic field produced by two magnetized iron bars where the exact analytical expression for the magnetic field is known and also they are applied to the same field data when a small amount of noise is superimposed. And, finally, they are applied to the measured magnetic field of the K1200 superconducting cyclotron.

1. INTRODUCTION

In doing orbit calculations for cyclotrons, it is sometimes necessary to construct off-median plane field components when only a discrete median plane map of the magnetic field is given (in the case of cyclotrons, data are usually measured on a polar mesh). Assuming median plane symmetry and using a fourth-order vector potential, the components of the magnetic field off the median plane [1] are given by

$$B_z = B(r, \theta) - \frac{z^2}{2!}\nabla_2^2 B(r, \theta) + \frac{z^4}{4!}\nabla_2^4 B(r, \theta), \tag{1}$$

$$B_r = \frac{\partial}{\partial r} C(r, \theta, z), \tag{2}$$

$$B_\theta = \frac{\partial}{r\partial\theta} C(r, \theta, z), \tag{3}$$

where B_z, B_r, and B_θ are magnetic field components in cylindrical polar coordinates and where

$$C(r, \theta, z) = zB(r, \theta) - \frac{z^3}{3!}\nabla_2^2 B(r, \theta)$$

and

$$B(r, \theta) = B_z(r, \theta, z = 0).$$

Here, ∇_2^2 is the two-dimensional Laplacian operator. Of course this truncated series easily can be extended to any order desired.

Gordon and Taivassalo [1, 2] evaluated coefficients using the second-order central difference schemes,

$$f_i' = (f_{i+1} - f_{i-1})/2\Delta \tag{4}$$

$$f_i'' = (f_{i+2} + f_{i-2} - 2f_i)/4\Delta^2, \tag{5}$$

where $f_i = f(x_i)$ and Δ is the step size of the mesh. This scheme presented difficulties both in accuracy and maximum order of expansion due to the amplified noise produced by taking derivatives. The differentiator ∇_2^2 should be applied successively to get higher order coefficients of the Taylor series. Differentiation amplifies the high frequency signals considerably which contain noise from various sources. If an effective suppression of the high frequency signals is not achieved, successive differentiation will soon destroy the significance of the data obtained so. The differentiator should also evaluate accurately the derivatives of signals over a sufficiently wide range of low frequency. This suggests that a compromise between these two conditions should be achieved.

A finite difference scheme which is a special case of a compact finite difference scheme is used to avoid the additional complexity imposed by compact schemes. If one wants to enhance the accuracy, a plausible way would be to use compact finite difference schemes. A lot of work has been done for compact finite difference schemes [3–6], and work for nonuniform mesh has also been done [7, 8]. Especially, Lele [6] did recent work on compact finite difference schemes. Even though the operators designed by Lele have a frequency response reasonably close to that of an ideal differentiator over $[0, \pi]$, they are not adequate for processing measured data containing noise because sufficient suppression of the high frequency signals is not provided. This is described in Section 6.

There are two possible ways to the compute derivatives of

* Work supported by the National Science Foundation under Grant No. Phy. 92-14992.

0021-9991/95 $6.00

a magnetic field. One way to do so is to process a magnetic field with a certain filter to remove the high frequency components before taking any derivatives. If the undesirable high frequency components are suppressed to a satisfactory extent, comparatively simple and standard differentiators could be used for computing the derivatives. The other way is to mix the processes of computing derivatives and filtering. We decided to take the latter approach because of the following reasons, even though we know that we are taking a rather complex approach. First of all, there are many orbit codes used in this laboratory to calculate various linear orbit properties which do not require any of the off-median plane magnetic field components but the median plane field map itself and all the researchers in this laboratory prefer having the field data unaltered for orbit computations to making use of any artificially processed field data. Second, it is vital to preserve the consistency between the results obtained by the orbit codes using only the unprocessed median plane field map and those by the nonlinear orbit codes utilizing both the median plane field map and the off-median plane field components.

We will use a composite operator of more than two finite difference operators using only three nodes. In this case, use of separate algorithms to evaluate derivatives at the nodes near boundaries can be avoided by imposing simple conditions for each 3-node operator. The following property is useful to get the frequency response of the composite operator obtained.

Let us consider a composite operator of two linear operators $L_1 = \sum h_1(n) f_n$ and $L_2 = \sum h_2(m) g_m$ with the corresponding frequency responses H_1 and H_2. Then the frequency response of the composite operator of these two is $H_1 H_2$, which is independent of the ordering of the application of the linear operators. If you consider the properties of the Z transformation [9, 10], it is straightforward to verify the previous statements. We are going to use this for the design of the operators.

2. DESIGN OF THE FIRST- AND THE SECOND-ORDER DIFFERENTIATOR IN ONE DIMENSION

The standard second-order central difference scheme for an initial evaluation of derivatives, composed with a filter, is used to improve the frequency response of the differentiators. The use of such a filter is to provide a strong suppression of the high frequency signals and, by adjusting a parameter Q of the filter, to improve the low frequency response at the same time.

First of all, the filter F is introduced that transforms $\{f_n\}$ to $\{\hat{f}_n\}$, suppressing the high frequency signals. For the first- and second-order differentiators, the parameter Q is adjusted, respectively, to produce a reasonable result:

$$
\begin{aligned}
& f_n \quad \text{for } n = 0, \ldots, N+1 \\
& \Downarrow \\
& g_n = (f_{n-1} + 2f_n + f_{n+1})/4 \\
& g_0 = f_0, \quad g_{N+1} = f_{N+1} \\
& \Downarrow \\
& h_n = g_n - \frac{Q}{4}(g_{n-1} + g_{n+1} - 2g_n) \\
& h_0 = g_0, \quad h_{N+1} = g_{N+1} \\
& \Downarrow \\
& k_n = (h_{n-1} + 2h_n + h_{n+1})/4 \\
& k_0 = h_0, \quad k_{N+1} = h_{N+1} \\
& \Downarrow \\
& \hat{f}_n = k_n - \tfrac{1}{4}(k_{n-1} + k_{n+1} - 2k_n) \\
& \hat{f}_0 = k_0, \quad \hat{f}_{N+1} = k_{N+1}.
\end{aligned}
$$

The frequency response $H^{(F)}$ of the filter is

$$
H^{(F)}(\omega) = \left[\cos^2(\omega/2) + \frac{Q}{4}\sin^2(\omega)\right]\left[\cos^2(\omega/2) + \frac{1}{4}\sin^2(\omega)\right]. \tag{6}
$$

The proposed first-order differentiator is a combination of the central difference scheme (refer to Eq. (8)) and a filter. With the choice of $Q = 1.70$, a reasonable low frequency response was obtained for the first-order differentiator. More detailed discussion about the choice $Q = 1.70$ is given at the section for resolving efficiency. The operator $D^{(1)}$ which approximates first-order derivative $\{(d/dx)f(x_n)\}$ for $n = 1, \ldots, N$ from a given set of data $\{f_n = f(x_n)\}$ for $n = 0, \ldots, N+1$ is

$$
\begin{aligned}
& f_n \quad \text{for } n = 0, \ldots, N+1 \\
& \Downarrow \\
& d_n = (f_{n+1} - f_{n-1})/2\Delta \quad \text{for } n = 1, \ldots, N \\
& \Downarrow \\
& s_n = (d_{n+1} + 2d_n + d_{n-1})/4 \\
& s_1 = d_1, \quad s_N = d_N \\
& \Downarrow \\
& g_n = s_n - \tfrac{1.7}{4}(s_{n+1} + s_{n-1} - 2s_n) \\
& g_1 = s_1, \quad g_N = s_N \\
& \Downarrow \\
& h_n = (g_{n+1} + 2g_n + g_{n-1})/4 \\
& h_1 = g_1, \quad h_N = g_N \\
& \Downarrow
\end{aligned}
$$

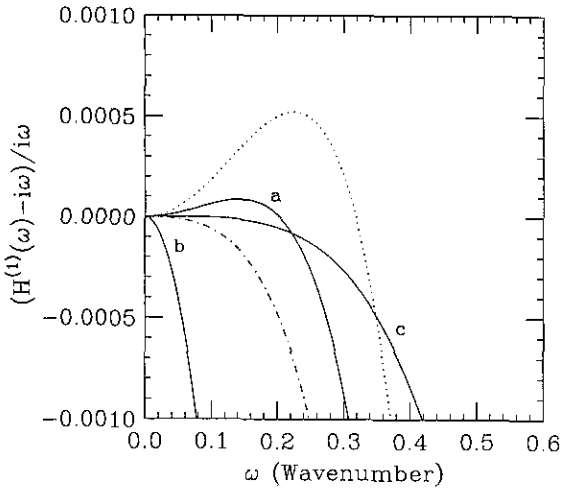

FIG. 1. Shows $(H^{(1)}(\omega) - i\omega)/i\omega$ for the second-order central difference scheme (real line "b"), that for the fourth-order central difference scheme (real line "c"), and that for the proposed differentiator (real line "a" with $Q = 1.70$). The dot-dash line corresponds to $Q = 1.65$ and the dotted line to $Q = 1.75$.

$$\frac{d}{dx} f(x_n) = h_n - \frac{1}{4}(h_{n+1} + h_{n-1} - 2h_n)$$

$$\frac{d}{dx} f(x_1) = h_1, \quad \frac{d}{dx} f(x_N) = h_N.$$

A complete expression of the operator $D^{(1)}$ is applied for the nodes with $n = 5$ to $n = N - 4$, but we can still get a good evaluation of derivatives for the rest of nodes at the same time. It is convenient to express an operator as a composition of several 3-node linear operators with a simple treatment of the nodes at the end. This saves us the trouble of using a separate algorithm to evaluate the derivatives at each of the nodes with $n = 1, ..., 4$ and $n = N - 3, ..., N + 1$.

The frequency response $H^{(1)}$ of the first-order differential operator, $D^{(1)}$, is

$$H^{(1)}(\omega) = i \sin(\omega)[\cos^2(\omega/2) + \tfrac{1.7}{4}\sin^2(\omega)] \times [\cos^2(\omega/2) + \tfrac{1}{4}\sin^2(\omega)]. \tag{7}$$

Note that this is purely imaginary, so it does not have any phase shift. Additionally it has a frequency response reasonably close to that of an ideal differentiator for low frequencies, and suppresses the high frequency signals sufficiently. Fractional differences of the frequency responses for several schemes are depicted in Fig. 1. By composing the second-order central difference scheme with the filter, the low frequency response was improved considerably, compared with that of the second-order central difference scheme alone (refer to Fig. 1).

Before making comparisons with any other schemes, let us define resolving efficiency of approximate first-order differentiators, $e_1(\varepsilon) \equiv \omega_f/\pi$ [6]. The value ω_f is the maximum wavenumber of a well-resolved wave satisfying the error tolerance relation $|H^{(1)}(\omega) - i\omega|/\omega \leq \varepsilon$ for any given positive value of ε. The resolution characteristics of several schemes are tabulated in Table I. In this paper, $Q = 1.70$ was chosen to maximize the resolving efficiency for $\varepsilon = 1.0 \times 10^{-4}$ (refer to Fig. 1). If one wants to maximize the resolving efficiency for $\varepsilon = 5.2 \times 10^{-4}$, the natural choice would be $Q = 1.75$ (refer to Fig. 1). According to Fig. 1 and Table I, the approximate first-order differentiation scheme is better than the second-order central difference scheme and worse than the fourth-order central difference scheme for low frequency signals. On the other hand, it is superior to them in suppressing the high frequency signals (refer to Fig. 2).

TABLE I

Resolving Efficiency $e_1(\varepsilon)$ of the First Derivative Schemes

Scheme	$\varepsilon = 0.1$	$\varepsilon = 0.01$	$\varepsilon = 0.001$
Newly designed first differentiator	0.29	0.16	0.10
Second-order central difference scheme	0.25	0.08	0.02
Fourth-order central difference scheme	*0.44*	*0.23*	*0.13*

The reason the second-order central difference scheme is used as an initial operator is that it is the simplest one. If one wants to use the more complicated fourth-order central difference scheme as an initial operator, one should also use more elaborate filters that have comparable resolving efficiency

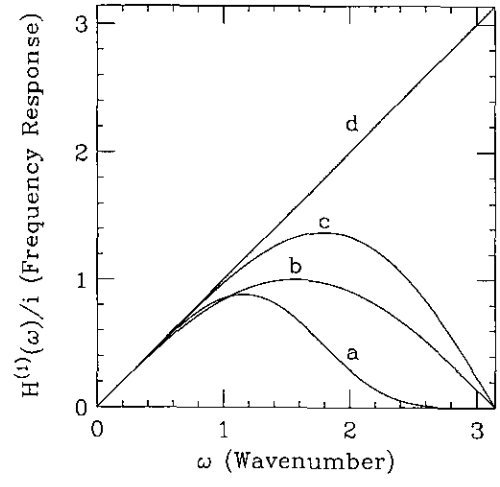

FIG. 2. Shows the frequency response divided by i, $H^{(1)}(\omega)/i$, as a function of the wavenumber ω. Curve "a" is for our proposed differentiator, curve "b" for the second order central difference scheme, curve "c" for the fourth-order central difference scheme, and curve "d" for the mathematical first-order differentiator. "a" is superior to "b" and "c" in suppressing high frequency signals and shows a frequency response reasonably close to that of the mathematical differentiator for low frequency as well.

(see Section 3). At present, these added complications do not seem necessary for our purposes. Here the second-order and the fourth-order central difference schemes for first-order derivatives are defined as

$$f_i' = (f_{i+1} - f_{i-1})/2\Delta \tag{8}$$

$$f_i' = \tfrac{4}{3}(f_{i+1} - f_{i-1})/2\Delta - \tfrac{1}{3}(f_{i+2} - f_{i-2})/4\Delta, \tag{9}$$

where $f_i = f(x_i)$ and Δ is the step size of the mesh.

The proposed second-order differentiator is a combination of the central difference scheme (refer to Eq. (11)) and a filter. With the choice of $Q = 1.36$, a reasonable low frequency response was obtained for the second-order differentiator. More detailed discussion about the choice $Q = 1.36$ is given in the section for resolving the efficiency. The operator $D^{(2)}$ that approximates second-order derivatives $\{(d^2/dx^2)f(x_n)\}$ for $n = 1, ..., N$ from a given set of data $\{f_n\}$ for $n = 0, ..., N + 1$ is given below:

$$f_n \quad \text{for } n = 0, ..., N+1$$

$$\Downarrow$$

$$d_n = (f_{n+1} + f_{n-1} - 2f_n)/\Delta^2 \quad \text{for } n = 1, ..., N$$

$$\Downarrow$$

$$s_n = (d_{n+1} + 2d_n + d_{n-1})/4$$

$$s_1 = d_1, \quad s_N = d_N$$

$$\Downarrow$$

$$g_n = s_n - \frac{1.36}{4}(s_{n+1} + s_{n-1} - 2s_n)$$

$$g_1 = s_1, \quad g_N = s_N$$

$$\Downarrow$$

$$h_n = (g_{n+1} + 2g_n + g_{n-1})/4$$

$$h_1 = g_1, \quad h_N = g_N$$

$$\Downarrow$$

$$\frac{d^2}{dx^2} f(x_n) = h_n - \frac{1}{4}(h_{n+1} + h_{n-1} - 2h_n)$$

$$\frac{d^2}{dx^2} f(x_1) = h_1, \quad \frac{d^2}{dx^2} f(x_N) = h_N.$$

The frequency response $H^{(2)}$ of the second-order differential operator, $D^{(2)}$, is

$$H^{(2)}(\omega) = -4\sin^2(\omega/2)[\cos^2(\omega/2) + \tfrac{1.36}{4}\sin^2(\omega)] \times [\cos^2(\omega/2) + \tfrac{1}{4}\sin^2(\omega)]. \tag{10}$$

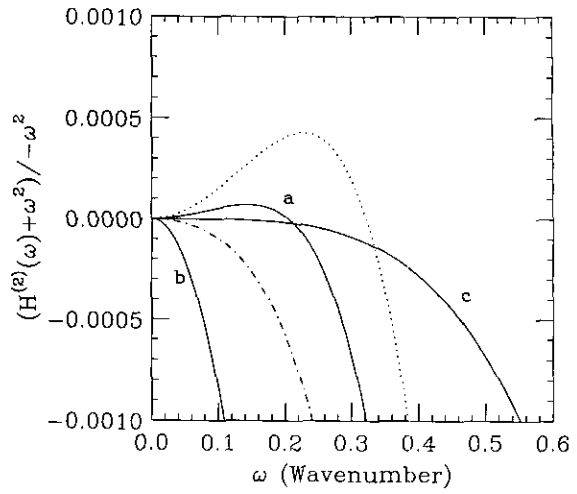

FIG. 3. Shows $(H^{(2)}(\omega) + \omega^2)/-\omega^2$ for the second-order central difference scheme (real line "b"), that for the fourth-order central difference scheme (real line "c"), and that for the proposed differentiator (real line "a" with $Q = 1.36$). The dot-dash line corresponds to $Q = 1.30$ and the dotted line to $Q = 1.40$.

Note that this is purely real, so it does not have any phase shift. The fractional differences of frequency response for several schemes are depicted in Fig. 3. By composing the standard central difference scheme with the filter, the low frequency response was improved considerably, compared with that of the second-order central difference scheme alone (refer to Fig. 3).

In a similar way, let us define a resolving efficiency of approximate second-order differentiators, $e_2 \equiv \omega_f/\pi$, where the value ω_f is the maximum wave-number of a well-resolved wave satisfying the tolerance relation $|H^{(2)} + \omega^2|/\omega^2 \leq \varepsilon$ for any given value of ε. In this paper, $Q = 1.36$ was chosen to maximize the resolving efficiency for $\varepsilon = 1.0 \times 10^{-4}$ (refer to Fig. 3). If one wants to maximize the resolution characteristics for $\varepsilon = 4.3 \times 10^{-4}$, the natural choice would be $Q = 1.40$ (refer to Fig. 3). The resolving efficiency for several schemes are tabulated in Table II. The approximate second-order differentiation scheme is better than the second-order central difference scheme and worse than the fourth-order central difference scheme for low frequency signals (refer to Fig. 3 and Table II). On the other hand, it is superior to them in suppressing high frequency

TABLE II

Resolving Efficiency $e_2(\varepsilon)$ of the Second Derivative Scheme

Scheme	$\varepsilon = 0.1$	$\varepsilon = 0.01$	$\varepsilon = 0.001$
Newly designed second differentiator	0.30	0.17	0.10
Second-order central difference scheme	0.35	0.11	0.03
Fourth-order central difference scheme	0.59	0.31	0.17

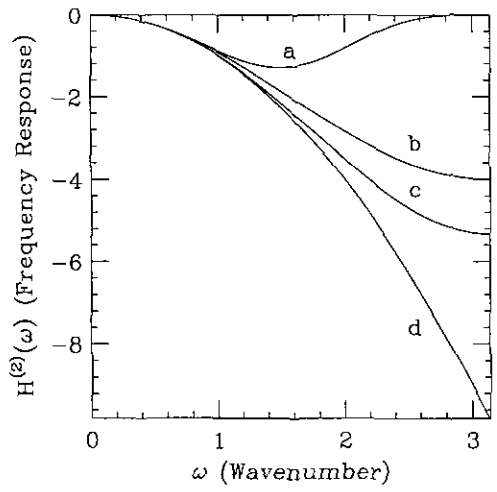

FIG. 4. Shows the frequency response $H^{(2)}(\omega)$ as a function of the wavenumber ω. Curve "a" is for our proposed second-order differentiator, curve "b" for the second-order central difference scheme, curve "c" for the fourth-order central difference scheme, and curve "d" for the mathematical second-order differentiator. "a" is superior to "b" and "c" in suppressing high frequency signals and shows a low frequency response reasonably close to that of the mathematical differentiator as well. Note that "b" and "c" do not suppress high frequency signals, and the effect shows up when they are applied to data containing noise.

signals (refer to Fig. 4). Here the second-order and the fourth-order central difference schemes are defined as

$$f_i'' = (f_{i+1} + f_{i-1} - 2f_i)/\Delta^2 \tag{11}$$

$$f_i'' = \tfrac{4}{3}(f_{i+1} + f_{i-1} - 2f_i)/\Delta^2 - \tfrac{1}{3}(f_{i+2} + f_{i-2} - 2f_i)/4\Delta^2, \tag{12}$$

where $f_i = f(x_i)$ and Δ is the step size of the mesh.

The reason why Gordon and Taivassalo [1, 2] used Eq. (5) instead of Eq. (11) or Eq. (12) is that the frequency response of Eq. (5) at $\omega = \pi$ is equal to 0 while those of Eq. (11) or Eq. (12) are not equal to 0 (refer to Fig. 4). Due to this, neither Eq. (11) nor Eq. (12) properly suppresses the high frequency signals, which makes it difficult to apply these schemes successively to get higher order derivatives of data with noise. Loss of the significance of data due to amplified noise is made clear by comparing Fig. 9, where a scheme, Eq. (11), that poorly suppresses high frequency signals is used and Fig. 10, where the proposed scheme with the noise filter is used.

3. DESIGN OF THE FIRST- AND THE SECOND-ORDER DIFFERENTIAL OPERATORS IN TWO-DIMENSIONAL CARTESIAN COORDINATES

For the partial differentiators in two dimensions, the second-order central difference schemes (Eq. (8) or Eq. (11)) with a filter in x and a filter in y are used. For the sake of convenience, the x filter will be called a "longitudinal filter" and the y filter will be called a "vertical filter" when a partial derivative with respect to x is taken. Differential operators in two dimensions are a simple generalization of the corresponding one-dimensional analogues with one difference. The difference is the addition of a "vertical filter" such that when partial differentiation with respect to x (y) is performed, suppression of the high frequency signals with respect to y (x) should be performed at the same time such that the low frequency signals pass through and a strong suppression of the high frequency signals is provided. This ensures the suppression of noise signals when the partial differential operators are applied successively to get the higher order derivatives. The importance of this filter is very well demonstrated in Table VI and Figs. 10 and 11.

The filter F_y that transforms $\{f_{n,m}\}$ to $\{\hat{f}_{n,m}\}$ suppressing the high frequency signals with respect to y with a choice of $Q = 1.01$ is given below:

$$f_{n,m} \quad \text{for } n = 0, \ldots, N+1;\ m = 0, \ldots, M+1$$

$$\Downarrow$$

$$g_{n,m} = (f_{n,m-1} + 2f_{n,m} + f_{n,m+1})/4$$

$$g_{n,0} = f_{n,0}, \quad g_{n,M+1} = f_{n,M+1}$$

$$\Downarrow$$

$$h_{n,m} = g_{n,m} - \tfrac{1.01}{4}(g_{n,m-1} + g_{n,m+1} - 2g_{n,m})$$

$$h_{n,0} = g_{n,0}, \quad h_{n,M+1} = g_{n,M+1}$$

$$\Downarrow$$

$$k_{n,m} = (h_{n,m-1} + 2h_{n,m} + h_{n,m+1})/4$$

$$k_{n,0} = h_{n,0}, \quad k_{n,M+1} = h_{n,M+1}$$

$$\Downarrow$$

$$\hat{f}_{n,m} = k_{n,m} - \tfrac{1}{4}(k_{n,m-1} + k_{n,m+1} - 2k_{n,m})$$

$$\hat{f}_{n,0} = k_{n,0}, \quad \hat{f}_{n,M+1} = k_{n,M+1}.$$

The frequency response $H_y^{(F)}$ of the filter, F_y, with $Q = 1.01$ is

$$H_y^{(F)}(\omega_x, \omega_y) = [\cos^2(\omega_y/2) + \tfrac{1.01}{4}\sin^2(\omega_y)] \times [\cos^2(\omega_y/2) + \tfrac{1}{4}\sin^2(\omega_y)], \tag{13}$$

and Fig. 5 shows the plot of this frequency response.

Let us define a resolving efficiency of the filter, $e_F \equiv \omega_f/\pi$, where the value ω_f is the maximum wave-number of a well-resolved wave satisfying the tolerance relation $|H^{(F)} - 1| \leq \varepsilon$; $e_F(\varepsilon = 0.1) = 0.32$, $e_F(\varepsilon = 0.01) = 0.17$, and $e_F(\varepsilon = 0.001) = 0.10$.

A first-order partial differentiator with respect to x is considered. A combination of the standard central difference scheme (refer to Eq. (8)) and an x filter (with $Q = 1.70$) and a y filter

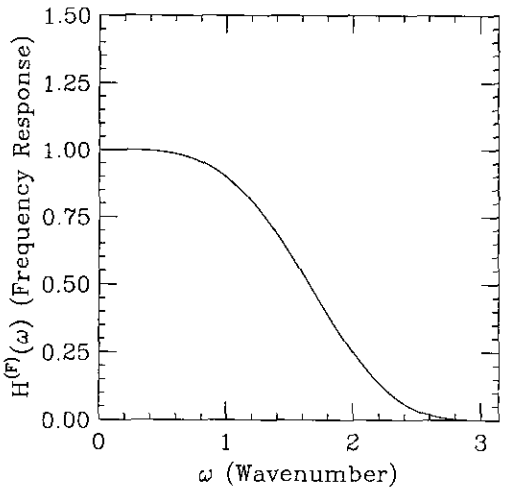

FIG. 5. Shows the frequency response, $H^{(F)}(\omega)$, of the filter used for the proposed partial differentiators as a function of wavenumber, ω. Good low-frequency response and suppression of high-frequency signals are shown.

(with $Q = 1.01$) are used. In this case, the x filter will be called the "longitudinal filter" and the y filter the "vertical filter." The differential operator $D_x^{(1)}$ that approximates the first-order partial derivatives with respect to x, $\{(\partial/\partial x)f(x_n, y_m)\}$ for $n = 1, ..., N$ and $m = 0, ..., M + 1$ from the data $\{f_{n,m} = f(x_n, y_m)\}$ for $n = 0, ..., N + 1$ and $m = 0, ..., M + 1$ is

$$
\begin{aligned}
& f_{n,m} \quad \text{for } n = 0, ..., N+1;\ m = 0, ..., M+1 \\
& \Downarrow \\
& d_{n,m} = (f_{n+1,m} - f_{n-1,m})/2\Delta_x \\
& \text{for } n = 1, ..., N;\ m = 0, ..., M+1 \\
& \Downarrow \\
& sx_{n,m} = (d_{n+1,m} + 2d_{n,m} + d_{n-1,m})/4 \\
& sx_{1,m} = d_{1,m}, \quad sx_{N,m} = d_{N,m} \\
& \Downarrow \\
& gx_{n,m} = sx_{n,m} - \tfrac{1.7}{4}(sx_{n+1,m} + sx_{n-1,m} - 2sx_{n,m}) \\
& gx_{1,m} = sx_{1,m}, \quad gx_{N,m} = sx_{N,m} \\
& \Downarrow \\
& hx_{n,m} = (gx_{n+1,m} + 2gx_{n,m} + gx_{n-1,m})/4 \\
& hx_{1,m} = gx_{1,m}, \quad hx_{N,m} = gx_{N,m} \\
& \Downarrow \\
& kx_{n,m} = hx_{n,m} - \tfrac{1}{4}(hx_{n+1,m} + hx_{n-1,m} - 2hx_{n,m}) \\
& kx_{1,m} = hx_{1,m}, \quad kx_{N,m} = hx_{N,m} \\
& \Downarrow
\end{aligned}
$$

$$
\begin{aligned}
& sy_{n,m} = (kx_{n,m+1} + 2kx_{n,m} + kx_{n,m-1})/4 \\
& sy_{n,0} = kx_{n,0}, \quad sy_{n,M+1} = kx_{n,M+1} \\
& \Downarrow \\
& gy_{n,m} = sy_{n,m} - \tfrac{1.01}{4}(sy_{n,m+1} + sy_{n,m-1} - 2sy_{n,m}) \\
& gy_{n,0} = sy_{n,0}, \quad gy_{n,M+1} = sy_{n,M+1} \\
& \Downarrow \\
& hy_{n,m} = (gy_{n,m+1} + 2gy_{n,m} + gy_{n,m-1})/4 \\
& hy_{n,0} = gy_{n,0}, \quad hy_{n,M+1} = gy_{n,M+1} \\
& \Downarrow \\
& \frac{\partial}{\partial x} f(x_n, y_m) = hy_{n,m} - \tfrac{1}{4}(hy_{n,m+1} + hy_{n,m-1} - 2hy_{n,m}) \\
& \frac{\partial}{\partial x} f(x_n, y_0) = hy_{n,0}, \quad \frac{\partial}{\partial x} f(x_n, y_{M+1}) = hy_{n,M+1},
\end{aligned}
$$

where Δ_x is the step size of the x-mesh.

Evaluation of derivatives at the nodes near boundaries is handled properly and with simplicity without introducing additional algorithms to handle them. In a similar way, the approximate first-order partial differentiator $D_y^{(1)}$ with respect to y can be obtained. The corresponding frequency response of $D_x^{(1)}$ is

$$
\begin{aligned}
H_x^{(1)}(\omega_x, \omega_y) = i \sin(\omega_x)[\cos^2(\omega_x/2) + \tfrac{1.7}{4}\sin^2(\omega_x)] \\
\times [\cos^2(\omega_x/2) + \tfrac{1}{4}\sin^2(\omega_x)] \\
\times [\cos^2(\omega_y/2) + \tfrac{1.01}{4}\sin^2(\omega_y)] \\
\times [\cos^2(\omega_y/2) + \tfrac{1}{4}\sin^2(\omega_y)],
\end{aligned}
\tag{14}
$$

and Fig. 6 shows the plot of the frequency response in the

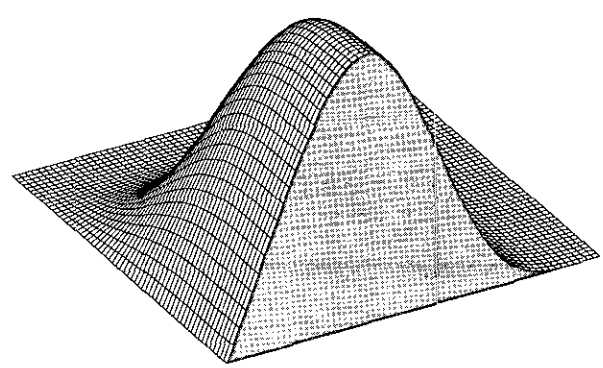

FIG. 6. Shows the frequency response of the first-order partial differentiator with respect to x divided by i, $H_x^{(1)}(\omega_x, \omega_y)/i$ for $0 \le \omega_x \le \pi$ and $0 \le \omega_y \le \pi$. Suppression of the high frequency signals both in x and y should be noted. It also shows good linear behavior for low frequency.

frequency domain. It should be noted that because this is purely imaginary there is not any phase shift.

A second-order partial differentiator with respect to x is considered. The standard central difference scheme (refer to Eq. (11)) composed with an x filter (with $Q = 1.36$) and a y filter (with $Q = 1.01$) is used. In this case, the x filter is called the "longitudinal filter" and the y filter is called the "vertical filter." The differential operator $D_x^{(2)}$ that approximates the second-order partial differentiation $\{(\partial^2/\partial x^2)f(x_n, y_m)\}$ with respect to x for $n = 1, ..., N$ and $m = 0, ..., M + 1$ from the data $\{f_{n,m} = f(x_n, y_m)\}$ for $n = 0, ..., N + 1$ and $m = 0, ..., M + 1$ is

$$
\begin{aligned}
&f_{n,m} \quad \text{for } n = 0, ..., N+1;\ m = 0, ..., M+1\\
&\Downarrow\\
&d_{n,m} = (f_{n+1,m} + f_{n-1,m} - 2f_{n,m})/\Delta^2\\
&\text{for } n = 1, ..., N;\ m = 0, ..., M+1\\
&\Downarrow\\
&sx_{n,m} = (d_{n+1,m} + 2d_{n,m} + d_{n-1,m})/4\\
&sx_{1,m} = d_{1,m}, \quad sx_{N,m} = d_{N,m}\\
&\Downarrow\\
&gx_{n,m} = sx_{n,m} - \tfrac{1.36}{4}(sx_{n+1,m} + sx_{n-1,m} - 2sx_{n,m})\\
&gx_{1,m} = sx_{1,m}, \quad gx_{N,m} = sx_{N,m}\\
&\Downarrow\\
&hx_{n,m} = (gx_{n+1,m} + 2gx_{n,m} + gx_{n-1,m})/4\\
&hx_{1,m} = gx_{1,m}, \quad hx_{N,m} = gx_{N,m}\\
&\Downarrow\\
&kx_{n,m} = hx_{n,m} - \tfrac{1}{4}(hx_{n+1,m} + hx_{n-1,m} - 2hx_{n,m})\\
&kx_{1,m} = hx_{1,m}, \quad kx_{N,m} = hx_{N,m}\\
&\Downarrow\\
&sy_{n,m} = (kx_{n,m+1} + 2kx_{n,m} + kx_{n,m-1})/4\\
&sy_{n,0} = kx_{n,0}, \quad sy_{n,M+1} = kx_{n,M+1}\\
&\Downarrow\\
&gy_{n,m} = sy_{n,m} - \tfrac{1.01}{4}(sy_{n,m+1} + sy_{n,m-1} - 2sy_{n,m})\\
&gy_{n,0} = sy_{n,0}, \quad gy_{n,M+1} = sy_{n,M+1}\\
&\Downarrow\\
&hy_{n,m} = (gy_{n,m+1} + 2gy_{n,m} + gy_{n,m-1})/4\\
&hy_{n,0} = gy_{n,0}, \quad hy_{n,M+1} = gy_{n,M+1}\\
&\Downarrow\\
&\frac{\partial^2}{\partial x^2} f(x_n, y_m) = hy_{n,m} - \tfrac{1}{4}(hy_{n,m+1} + hy_{n,m-1} - 2hy_{n,m})
\end{aligned}
$$

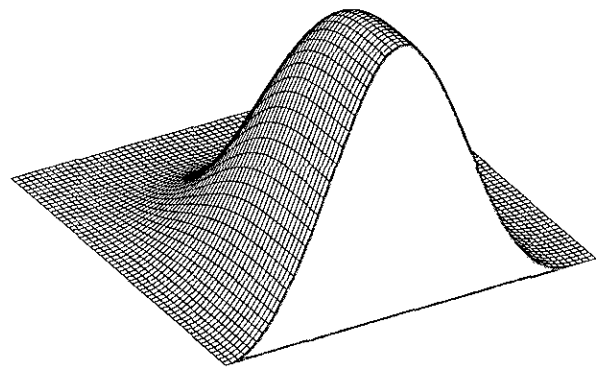

FIG. 7. Shows the frequency response of the second-order partial differentiator with respect to x multiplied by -1, $H_x^{(2)}(\omega_x, \omega_y)$ for $0 \le \omega_x \le \pi$ and $0 \le \omega_y \le \pi$. Suppression of the high frequency signals both in x and y should be noted. It shows good quadratic behavior for low frequency signals as well.

$$\frac{\partial^2}{\partial x^2} f(x_n, y_0) = hy_{n,0}, \quad \frac{\partial^2}{\partial x^2} f(x_n, y_{M+1}) = hy_{n,M+1},$$

where Δ_x is the step size of the x-mesh.

The approximate second-order partial differentation $D_y^{(2)}$ with respect to y can be obtained in a similar way. The corresponding frequency response of $D_x^{(2)}$ is

$$
\begin{aligned}
H_x^{(2)}(\omega_x, \omega_y) = &-4\sin^2(\omega_x/2)[\cos^2(\omega_x/2) + \tfrac{1.36}{4}\sin^2(\omega_x)]\\
&\times [\cos^2(\omega_x/2) + \tfrac{1}{4}\sin^2(\omega_x)]\\
&\times [\cos^2(\omega_y/2) + \tfrac{1.01}{4}\sin^2(\omega_y)]\\
&\times [\cos^2(\omega_y/2) + \tfrac{1}{4}\sin^2(\omega_y)]
\end{aligned}
\tag{15}
$$

and Fig. 7 shows the plot of the frequency response in the frequency domain.

4. DESIGN OF THE OPERATOR FOR THE TWO-DIMENSIONAL LAPLACIAN OPERATOR IN POLAR COORDINATE SYSTEM

Special caution should be taken when we deal with the Laplacian operator in polar coordinates because the operator is

$$\nabla_2^2 = \frac{\partial^2}{\partial r^2} + \frac{\partial}{r\partial r} + \frac{\partial^2}{r^2\partial\theta^2}, \tag{16}$$

which is a multiplication of a partially differentiated function and $1/r$ or $1/r^2$.

In this case, the three terms should be processed separately and then added together to compute $\nabla_2^2 f$. The term $(\partial^2/\partial r^2)f(r_n, \theta_m)$ on a polar mesh is straightforward to compute because it is not multiplied by an additional function of r or θ. For the rest of the terms, $(\partial/\partial r)f(r_n, \theta_m)$ and $(\partial^2/\partial\theta^2)f(r_n, \theta_m)$ should

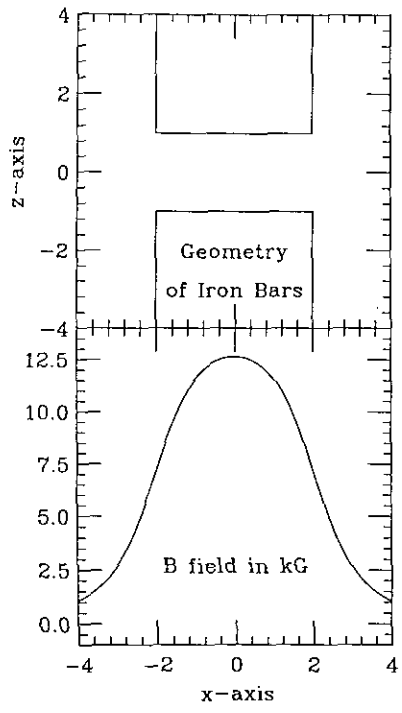

FIG. 8. Shows a cross-sectional view of the geometry of the iron bars in the plane $y = 0$, and the field values B_z $(x, y = 0, z = 0)$ in *kG*. Note how fast the field values decrease as a function of x. The maximum field value is 12.6 *kG*.

be computed first and then multiplied by the corresponding $1/r_n$ and $1/r_n^2$, respectively. After completing the processing of the three individual terms, they should be summed to get the result of $\nabla_2^2 f$. In any other coordinate system, the same rule is applied.

5. APPLICATION TO THE FIELD PRODUCED BY MAGNETIZED IRON BARS

Two long iron bars were considered with the geometry $-2 \leq x \leq 2$, $-2 \leq y \leq 2$, and $z \geq 1$ for one iron bar and $-2 \leq x \leq 2$, $-2 \leq y \leq 2$, and $z \leq -1$ for the other (refer to Fig. 8). These bars are uniformly magnetized in the $+z$ direction with a resultant internal field B_s. Let us define $x_1 = -2$, $x_2 = 2$, $y_1 = -2$, and $y_2 = 2$. The magnetic field due to the two sheets of surface charge [1, 11] is given by

$$B_z(x, y, z) = \frac{B_s}{4\pi} \sum_{i,j} (-1)^{i+j} \left[\arctan\left(\frac{X_i Y_j}{Z_+ R_+}\right) + \arctan\left(\frac{X_i Y_j}{Z_- R_-}\right) \right], \tag{17}$$

where $i, j = 1, 2$, B_s is taken to be 21.4 *kG* [1],

$$X_i = x - x_i,$$

$$Y_j = y - y_j,$$

$$Z_+ = 1 + z,$$

$$Z_- = 1 - z,$$

$$R_\pm = (X_i^2 + Y_j^2 + Z_\pm^2)^{1/2}.$$

The geometry of the iron bars in the plane $y = 0$, and the field values of $B_z(x, y = 0, z = 0)$ in *kG* along the x-axis are shown in Fig. 8.

B_z is Taylor-expanded around $z = 0$ just as in Eq. (1). For the sake of convenience, let us define as in Section 2:

$$B(x, y) = B_z(x, y, z = 0). \tag{18}$$

The program "Mathematica" was used to obtain the analytical expressions of various derivatives such as $\nabla_2^2 B$, ..., $\nabla_2^6 B$ with $\nabla_2^2 = \partial^2/\partial x^2 + \partial^2/\partial y^2$.

We made comparisons between the results obtained from the analytically differentiated formulas using the program "Mathematica" and the results from the two different approximate second-order differential operators; one is $(f_{n+2} + f_{n-2} - 2f_n)/4\Delta^2$ used by Gordon and Taivassalo [1, 2] and the proposed differentiators described in Section 3. For the sake of convenience, let us call the former "operator 1" and the latter "operator 2."

The numerical calculations start with values of $B(x, y)$ stored in a uniform square mesh with $\Delta x = \Delta y = 0.05$. Data from $-4 \leq x \leq 4$ and $-4 \leq y \leq 4$ were chosen for comparison because this is the region where drastic changes occur. Exact evaluation of the derivatives of various orders was done by analytically differentiating Eq. (17) evaluated on the median plane, where $z = 0$ using the program "Mathematica." Numerical evaluation of the derivatives of various orders was done by applying the approximate differentiators to the field data of B. In obtaining the numerical evaluation of the derivatives, the field data expressed in *kG* up to the 11th decimal place obtained from Eq. (18) were used to keep the truncation error as small as possible.

In each case, we calculated the values of a particular term in the expansion of B_z for $z = 0.5$, which is halfway from the median plane to the poleface. The rms difference in *kG* between the values obtained from the two different approximation methods and the exact values from the analytically differentiated expressions are given at Table III, where rms(D) is the rms

TABLE III

	Operator 1	Operator 2
Term for comparison	rms(D)	rms(D)
$\nabla_2^2 B \times 0.5^2/2!$	1.36×10^{-3}	1.86×10^{-5}
$\nabla_2^4 B \times 0.5^4/4!$	1.02×10^{-3}	3.13×10^{-5}
$\nabla_2^6 B \times 0.5^6/6!$	0.481×10^{-3}	3.07×10^{-5}

TABLE IV

Term for comparison	Operator 1 rms(D)	Operator 2 rms(D)
$\nabla_2^2 B \times 0.5^2/2!$	5.34×10^{-3}	3.60×10^{-4}
$\nabla_2^4 B \times 0.5^4/4!$	3.79×10^{-3}	5.98×10^{-4}
$\nabla_2^6 B \times 0.5^6/6!$	1.59×10^{-3}	4.54×10^{-4}

difference between the numerical and analytical results. The largest magnitudes of the second-order, the fourth-order, and the sixth-order terms of expansion are 0.948 *kG*, 0.140 *kG*, and 0.0252 *kG*, respectively. $\nabla_2^2 B \times 0.5^2/2!$ is the second-order term in z evaluated at $z = 0.5$ when $B_z(x, y, z)$, Eq. (17), is Taylor-expanded with respect to z around the $z = 0$ plane, obtained by applying the second-order differentiator ∇_2^2 to the given data from B; $\nabla_2^4 B \times 0.5^4/4!$ is the fourth-order term in z evaluated at $z = 0.5$, obtained by applying the second-order differential operator ∇_2^2 twice to the given data; and $\nabla_2^6 B \times 0.5^6/6!$ is the sixth-order term in z evaluated at $z = 0.5$, obtained by applying ∇_2^2 three times to the given data.

Similar calculations were done with $\Delta x = 0.1$ and $\Delta y = 0.1$. The values of the rms differences in *kG* are tabulated at Table IV. The largest magnitudes of the second-order, the fourth-order, and the sixth-order terms of expansion are 0.948 *kG*, 0.140 *kG*, and 0.0252 *kG*, respectively. By comparing Table IV and Table III, we can see the effect of step size, or in other words, the effect of the sampling rate. In both cases, "operator 2" outperforms "operator 1."

6. APPLICATION TO DATA WITH NOISE

We assumed that noise in the data could be simulated by generating random numbers and adding them to the values of B stored in the square mesh described above. Comparison was then made between the results obtained from "operator 2" and "operator 1" to determine their characteristics when applied to data with noise. In order to compare the results with those in Table IV above, we used the same mesh spacing, $\Delta x = \Delta y = 0.1$. The random numbers added to the stored field data are within $\pm 1.00 \times 10^{-4}$ *kG*, which is around the limit of measurement accuracy. The rms difference between the field data, with and without this noise is 5.75×10^{-5} *kG* (which agrees quite well with the expected values, $(10/\sqrt{3}) \times 10^{-5}$ *kG*).

It should be noted that the magnitude of random noise is very small compared with the maximum field value of 12.6 *kG* (see Fig. 8) for the field described in Section 5, and yet its effect on the derivatives is not negligible at all. Table V shows the values of the rms differences between the two approximate differentiators and the analytically differentiated formulas. With noise, "operator 2" is superior to "operator 1." Approximate second-order differentiators such as Eq. (11) and Eq. (12)

TABLE V

Term for comparison	Operator 1 rms(D)	Operator 2 rms(D)
$\nabla_2^2 B \times 0.5^2/2!$	5.40×10^{-3}	0.682×10^{-3}
$\nabla_2^4 B \times 0.5^4/4!$	4.48×10^{-3}	1.74×10^{-3}
$\nabla_2^6 B \times 0.5^6/6!$	3.60×10^{-3}	2.08×10^{-3}

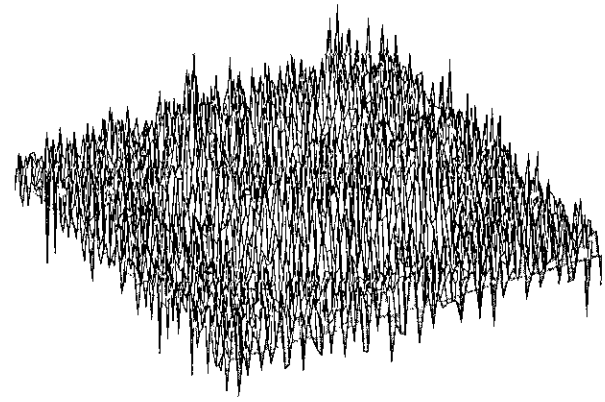

FIG. 9. Shows the fourth-order term, $\nabla_2^4 B \times 0.5^4/4!$, obtained by applying the second-order central difference scheme, Eq. (11), to the stored median plane data with random noise within $\pm 1.00 \times 10^{-4}$ *kG*, as described in Section 6. The data are stored in a square mesh with $-4 \le x \le 4$, $\Delta x = 0.1$, and $-4 \le y \le 4$, $\Delta y = 0.1$. The maximum value from this calculation and that from the analytical formula are 0.2311 *kG* and 0.1399 *kG*, respectively, and the corresponding minima are -0.1758 *kG* and -0.0865 *kG*, respectively. It is clear that without proper suppression of high frequency signals, it is difficult to get significant data. Compare with Fig. 10.

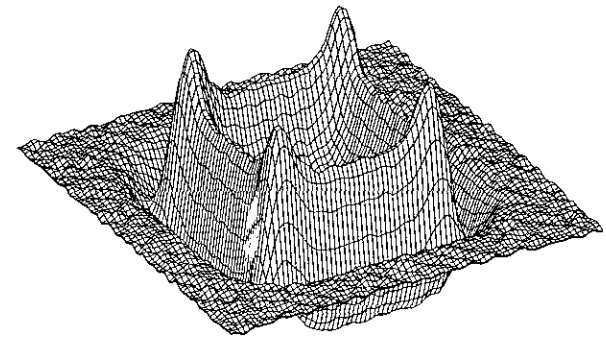

FIG. 10. Shows the results obtained from the same calculation as those depicted in Fig. 9, but with the use of the improved second-order differentiator and the "vertical filter" described in Section 3. The high frequency components observed are due to the random noise within $\pm 1.00 \times 10^{-4}$ *kG* added to the analytical field data to see the effects of noise. The maximum value from this calculation and that from the analytical formula are 0.1401 *kG* and 0.1399 *kG*, respectively, and the corresponding minima are -0.0895 *kG* and -0.0865 *kG*, respectively. Comparison with Fig. 9 makes clear the importance of suppressing high frequency signals.

TABLE VI

Term for comparison	With vertical filter rms(D)	Without vertical filter rms(D)
$\nabla_2^2 B \times 0.5^2/2!$	0.682×10^{-3}	0.962×10^{-3}
$\nabla_2^4 B \times 0.5^4/4!$	1.74×10^{-3}	3.33×10^{-3}
$\nabla_2^6 B \times 0.5^6/6!$	2.08×10^{-3}	5.53×10^{-3}

are inferior to "operator 1" when dealing with data with noise since the frequency response near $\omega = \pi$ is non-zero (see Fig. 4). The relative effectiveness of various differentiators in suppressing high frequency signals is very well shown in Figs. 9 and 10. The effect of adding noise can also be observed by comparing Tables V and IV which differ only in the addition of noise for Table V. The largest magnitudes of the second-order, fourth-order, and sixth-order terms are 0.948 kG, 0.140 kG, and 0.0252 kG, respectively.

As shown in Section 3, our approximate partial differentiators are accompanied by the "vertical filter" which filters data in the y (x) direction when partial derivatives are taken with respect to x (y). If the data contain no noise at all and are perfectly analytical, the "vertical filter" makes little difference. But it becomes indispensable when data with noise must be dealt with. Table VI shows the rms difference in kG between results obtained from "operator 2," with and without the "vertical filter." For the sake of convenience, let us call the former "with vertical filter" and the latter "without vertical filter." As can be seen from Table VI, the "vertical filter" becomes progressively more important with each succeeding term. Thus the "vertical filter" is indispensable for evaluating higher order derivatives of data with noise. Figures 10 and Fig. 11 show the fourth-order terms, one evaluated by the proposed second-order differentiators with the "vertical filter" in Section 3 and the other by the same differentiator without the "vertical filter." The contrast between the two becomes sharper for higher order derivatives. The largest magnitudes of the second-order, fourth-order, and sixth-order terms of expansion are 0.948 kG, 0.140 kG, and 0.0252 kG, respectively.

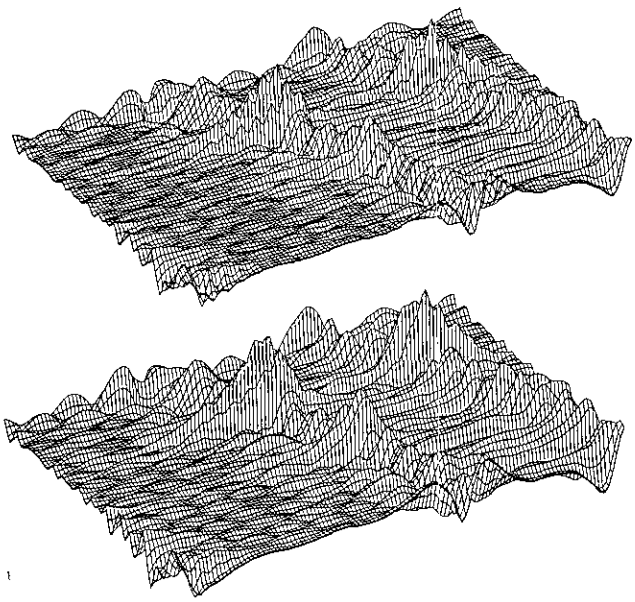

FIG. 12. Shows two maps of the fourth-order term in Eq. (1) evaluated at $z = 0.5$ (in), $\nabla_2^4 B \times 0.5^4/4!$ for a magnetic field with $q/A = 0.25$ and a nominal final energy $E_f = 40$ MeV/u of the K1200 superconducting cyclotron with 32 (in) $\leq r \leq 40$ (in) and $0° \leq \theta \leq 119°$ with the maximum field of 45.4 kG. The map at the top is obtained by using the differentiators in Eqs. (4), (5) and the map at the bottom by utilizing the proposed differentiators. The two maps are plotted to the same scale. The maximum and minimum values of the map at the top are (67.2 G, -82.0 G), respectively, while those of the map at the bottom are (82.3 G, -103.8 G), respectively. Clearly the magnitudes of the extremum values evaluated by the proposed differentiators are larger than those obtained by utilizing Eqs. (4), (5). This is an indication of the improved low-frequency characteristics. At the same time, the map at the bottom has a smoother surface compared with the map at the top, which is a result of effective high frequency filtering of the proposed differentiators.

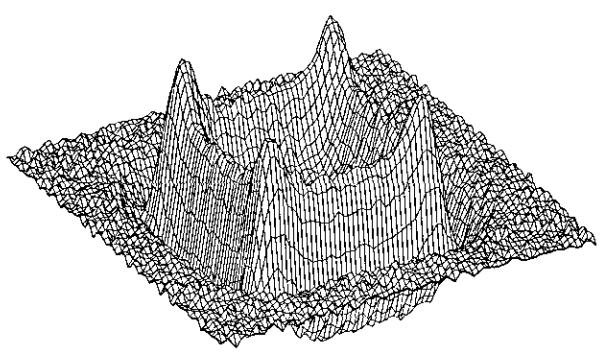

FIG. 11. Shows the same results as those depicted in Fig. 10, but here they were obtained without the use of the "vertical filter." The high frequency components observed are due to the random noise within $\pm 1.00 \times 10^{-4}$ kG added to the analytical field data to see the effects of noise. The maximum value from this calculation and that from the analytical formula are 0.1415 kG and 0.1399 kG, respectively, and the corresponding minima are -0.0928 kG and -0.0865 kG, respectively. It is clear that without the "vertical filter," suppression of high frequency signals is not sufficient. The "vertical filter" is indispensable to evaluate higher order derivatives.

7. APPLICATION TO THE MAGNETIC FIELD OF THE K1200 SUPERCONDUCTING CYCLOTRON

The K1200 superconducting cyclotron at National Superconducting Cyclotron Laboratory was designed to accelerate various heavy ions. The median plane field map is measured on the polar mesh with $\Delta\theta = 1°$ and $\Delta r = 0.1$ (in) while the radius of the machine is 42 (in). From the Fourier analysis, we can safely assume that the cutoff frequency $\omega_{\text{cutoff}} = 1.05$ which

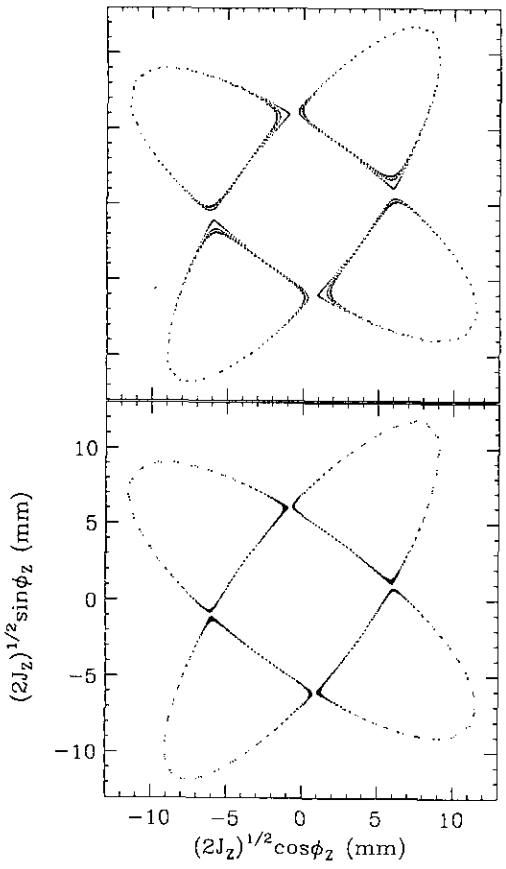

FIG. 13. Shows two maps of orbits close to the separatrix for $\nu_z = 0.740$ which is near the $\nu_z = \frac{3}{4}$ resonance at $E = 35.6$ MeV/u for a field with $q/A = 0.25$ and a nominal final energy $E_f = 40$ MeV/u of the K1200 superconducting cyclotron. J_z and ϕ_z are the action and angle variable. The orbits are computed for 400 turns with two different versions of the Z^4 orbit code. One is using the differentiators in Eqs. (4), (5) and the other is utilizing the proposed differentiators. Due to the chaotic layer on the separatrix, any kind of errors in computations can be visualized with ease. The map of the orbit computed by the Z^4 orbit code using the differentiators in Eqs. (4), (5) spirals inward (see the top figure) and is asymmetric, while that obtained by the Z^4 orbit code exhibits more physical behavior (see the bottom figure). This serves as indirect evidence for the reliability of the proposed differentiators as a tool for evaluating the off-median plane field components of cyclotrons.

corresponds to the 60th harmonic in our case. At the cutoff frequency, the fractional error of the proposed first-order differentiator is 16.9% and that of the proposed second-order differentiator 14.8%.

We now apply the proposed differentiators to evaluate the coefficients of the Taylor series in Eq. (1) for the median plane magnetic field data of the K1200 cyclotron. The magnetic field used as an example is for particles with $q/A = 0.25$ and a nominal final energy $E_f = 40$ MeV/u. As an illustration, two maps of the fourth-order term evaluated at $z = 0.5$ (in), $\nabla_2^4 B \times 0.5^4/4!$, are presented. The map at the top in Fig. 12 is obtained by using the differentiators in Eqs. (4), (5), used by Gordon and Taivassalo, and the map at the bottom in Fig. 12 by utilizing the proposed differentiators. First of all, the magnitudes of the maximum and the minimum are larger when the proposed differentiators are used, which is an indication of the improved low frequency characteristics. Second the surface of the map obtained by using the proposed differentiators is smoother, which proves the effective filtering of the high frequency components by the proposed differentiators. From the comparison, it can be deduced that the proposed differentiators do have the characteristics necessary in computing the off-median plane field components of cyclotrons.

As an indirect test, the results of orbit computation conducted near the $\nu_z = \frac{3}{4}$ resonance are presented [12]. An orbit quite near the separatrix was chosen where, due to the existence of chaotic layer, any kind of errors in the computation can easily be amplified. Figure 13 shows clearly the difference. The map of the orbit computed by the Z^4 orbit code using the differentiators in Eq. (4, 5) spirals inward and is asymmetric while that obtained by the Z^4 orbit code, making use of the proposed differentiators, exhibits more physical behavior. Besides this orbit, we ran several different orbits, even though they are not presented here. It turned out that the differentiators poorly suppressing high frequency components amplify the chaotic behavior of orbits near the chaotic region.

8. CONCLUSION

The low frequency characteristics of the approximate differentiators described in this paper are comparable to those of fourth-order central difference schemes. In particular, the resolving efficiency of our approximate differentiators is good enough to process data with maximum wave-number less than about 0.5.

In addition, our approximate differentiators sufficiently suppress high frequency signals. We have also found that the "vertical filter" suppressing high frequency signals in y (x) direction when taking partial derivatives with respect to x (y) plays an important role in obtaining higher order derivatives by successive application of the approximate differentiators. Our approximate differentiators are superior to the second-order central difference scheme and the fourth-order central difference scheme in dealing with data with noise.

The proposed differentiators might not be suitable for general purposes but they proved to be effective in computing the off-median plane field components using only the measured median plane field map of cyclotrons.

ACKNOWLEDGMENTS

I owe to Dr. M. M. Gordon the motivation of this work and deep thanks for helpful discussion and advice.

REFERENCES

1. M. M. Gordon and V. Taivassalo, *Nucl. Instrum. Methods A* **247,** 423 (1986).

2. M. M. Gordon and V. Taivassalo, *IEEE Trans. Nucl. Sci.* **NS-32,** 2447 (1985).
3. H. O. Kreiss, S. A. Orszag, and M. Israeli, *Annu. Rev. Fluid Mech.* **6,** 281 (1974).
4. R. S. Hirsh, *J. Comput. Phys.* **19,** 90 (1975).
5. Y. Adam, *J. Comput. Phys.* **24,** 10 (1977).
6. S. K. Lele, *J. Comput. Phys.* **103,** 16 (1992).
7. S. G. Rubin and P. K. Khosla, *J. Comput. Phys.* **24,** 217 (1977).
8. W. J. Goedheer and J. H. H. M. Potters, *J. Comput. Phys.* **61,** 269 (1985).
9. J. G. Proakis and D. G. Manolakis, *Introduction to Digital Signal Processing* (Macmillan, New York, 1988).
10. A. V. Oppenheim and R. W. Schafer, *Discrete-Time Signal Processing* (Prentice–Hall, Englewood Cliffs, NJ 1989), p. 149.
11. R. J. Thome and J. M. Tarrh, *MHD and Fusion Magnets* (Wiley, New York, 1982), p. 319.
12. D. Jeon and M. M. Gordon, *Nucl. Instrum. Methods A,* in press.